Intra-articular Administrated Hydrogels of Hyaluronic Acid Hybridized with Triptolide/Gold Nanoparticles for Targeted Delivery to Rheumatoid Arthritis Combined with Photothermal-chemo Therapy

Chenxi Li
Beijing University of Chinese Medicine
Rui Liu
Beijing University of Chinese Medicine
Yurong Song
Beijing University of Chinese Medicine
Dongjie Zhu
Beijing University of Chinese Medicine
Liuchunyang Yu
Beijing University of Chinese Medicine
Qingcai Huang
Beijing University of Chinese Medicine
Zhengjia Zhang
Beijing University of Chinese Medicine
Zeyu Xue
Beijing University of Chinese Medicine
Zhenglai Hua
Beijing University of Chinese Medicine
Cheng Lu
China Academy of Chinese Medical Sciences
Yuanyan Liu (yyliu_1980@163.com)
Beijing University of Chinese Medicine https://orcid.org/0000-0003-3840-5292

Research Article

Keywords: Triptolide, Rheumatoid arthritis, TP-Au/HA hybrid hydrogels, mTOR/p70S6K pathway, Chemo-photothermal treatment, NIR imaging

Posted Date: July 30th, 2021

DOI: https://doi.org/10.21203/rs.3.rs-750774/v1

Abstract

Triptolide (TP) as a disease-modifying anti-rheumatic drug (DMARD) is effective on the treatment of rheumatoid arthritis (RA). To alleviate the toxicity and elevate therapeutic specificity, hyaluronic acid (HA) hydrogels load RGD-attached gold nanoshell containing TP are synthesized, which can be used for targeted photothermal-chemo therapy, and imaging of RA in vivo. The hydrogels system composed of thiol and tyramine modified HA conjugates has been applied artificial tissue models of cartilage for studying drug delivery and release properties. After the degradation of HA chains, heat together with drugs can be delivered to the inflammatory joints simultaneously due to the near-infrared resonance (NIR) irradiation of Au nanoshell. RA is a chronic inflamed disease, which is characterized by synovial inflammation of multiple joints, and can be penetrated with NIR light. These intra-articular administrated hybrid hydrogels combined with NIR irradiation can improve clinical arthritic conditions and inflamed joints in collagen-induced arthritis (CIA) mice, which just need a smaller dosage of TP with non-toxicity. Additionally, the TP-Au/HA hybrid hydrogels treatment reduced the invasion and migration of RA fibroblast-like synoviocytes (RA-FLSs) in vitro significantly, through reducing the phosphorylation of mTOR and p70S6K, its substrates, and confirmed that the mTOR pathway was inhibited.

1. Introduction

Rheumatoid arthritis (RA) is a systematic inflamed disease, which is characterized by aggressive joint destruction and persistent synovitis [1]. The main treatment of RA is to use disease-modifying anti-rheumatic drugs (DMARDs), which can improve inflammatory conditions and delay progression [2]. As an epoxide diterpene lactone compound, TP has been used clinically to inhibit the expression of adhesion molecules, metalloproteinases, and pro-inflammatory cytokine, thus demonstrating anti-inflammatory and cartilage protective effects in the treatment of RA [3–5]. However, as a DMARD, due to its multiple organ toxicity, less solubility, low bioavailability, less stability, rapid excretion and non-specific targeting, its anti-arthritic efficacy was not fully exerted in clinical [6, 7]. Therefore, the novel delivery systems will be an effective tool for RA treatment, which maintain a higher concentration of TP in the main inflamed area of joints, and smaller-dosage administration is used to reduce side effects.

Recently, the combination of hydrogels and various NIR nanostructures is used in the fields of drug deliver, tissue regeneration, analgesia, chondroprotection, articular cartilage lubrication and anti-inflammation, these water-swollen and three-dimensional polymer networks have gained enormous attention [8–11]. Due to the advantages of moldability and less invasiveness during delivery, they can provide a favourable micro-environment for the growing, survival and proliferation of cells [6, 12]. When these hydrogels load nanoparticles can be released in a sustained manner, such as naked drug molecules, growth factors and other bioactive compounds, [13]. Especially, they can imitate the natural extracellular matrix (ECM) and have structural and mechanical properties similar to many tissues[12, 14]. As an important component of ECM, hyaluronic acid (HA) is extensively used in clinical treatments of RA due to its biodegradability, biocompatibility and non-immunogenicity [15]. HA contributes to joint

lubrication, provides a renewed source of HA for joint tissues, cushions the load transfer across articular surfaces and anti-inflammatory properties for synovial fluid [6, 16].

Through physically crosslinked or chemically modified improvement, HA based scaffolds, mechanically soft/tough hydrogels, in-situ hydrogels and viscoelastic solutions have been prepared successfully [6, 12]. However, most hydrogels may lead to the uncontrolled and rapid release of tiny bare molecules because of the high-water substance and large size of pore [17]. Particularly, hydrophobic drugs with less water-soluble lead to simply release precipitate or from the hydrogels rapidly [17]. Hybrid hydrogels has been synthesized to overcome the limitations, the delivery systems is the combination of drug-loaded nanoparticles with hydrogels [18]. Among various kinds of Au nanostructures, nanoshells, nanocages and nanorods, have attracted a potential interest in the various fields such as bio-sensors, drug delivery, imaging, tissue engineering and photothermal therapy [19–21]. Au nanostructures have good stability and biocompatibility, excellent properties of optics and electricity, and the easiness of surface modification in vivo [19, 22]. Meanwhile, Au nanostructures exhibit the unique surface plasmon resonance and intense absorption in NIR region, and due to its strong NIR absorption and localized cytotoxic heat upon NIR irradiation, allowing their use NIR absorbance imaging and photothermal therapy in vivo [19]. In vitro release studies have demonstrated that drug from the metallic nanoparticles hybrid higher cross-linked hydrogels have longer-sustained delivery [17]. These results show that drug delivery systems can be designed to provide a customized release rates and sustained delivery of drugs with appropriately designing of nanoparticles carriers and network structure.

For the treatment of RA, we developed TP-Au/HA hybrid hydrogels with RGD targeting, are directly intraarticular injected into CIA mice, which may potentially minimize side effects [9]. After the degradation of HA chains, TP-Au-RGD nanoparticles are exposed to the surrounding environment [23]. The accumulation of synthesized nanoparticles is enhanced in the inflammatory joints due to the TP-Au nanoparticles contain RGD peptides. Due to Au nanoshell, heat is generated and drugs are released from Poly (DL-lactic-co-glycolic acid) (PLGA)-TP nanoparticles rapidly upon NIR exposure, allow photothermally to control drug delivery and release. The application of hybrid hydrogels earns superior therapeutic effect compared to conventional treatment in CIA mice.

Furthermore, in vivo and in vitro experiments are applied to deeply verify the antirheumatic mechanisms of TP-Au/HA hybrid hydrogels. These synthesized hydrogels are specifically targeted to inflamed joints, and exert superior anti-arthritic effects on reducing destructive joint inflammation mediated by RA-FLSs with low toxicity [24, 25]. To reveal the mechanism of targeted drug delivery in inflammatory joints, RA-FLSs are applied for in-depth signaling pathway investigation, which for their characteristic pathogenic behaviors, such as mediate inflammation, aggressive phenotype and destruction of the joint [26]. It indicates that the anti-inflammatory effects of TP-Au/HA hybrid hydrogels on RA-FLSs are occurred by regulating the mTOR/p70S6K signal pathway. mTOR/p70S6K signal pathway is kept in an abnormally activated state, leading to the high expression of anti-apoptotic genes of downstream and then a subsequent influence on multiple effector molecules of downstream [27, 28]. Therefore, the study aims to

study the anti-inflammation effects of TP-Au/HA hybrid hydrogels in CIA mice and to reveal the signaling pathways that may be involved.

2. Material And Methods

2.1 Materials

SH-PEG-COOH (Mw = 5000) and TP were purchased from Shanghai yuanye Bio-Technology Co., Ltd. Hyaluronic acid (HA; from Cockscomb) was purchased from Aladdin. Cystamine dihydrochloride, Tyramine hydrochloride (TA), DL-dithiothreitol (DTT) and Sulfo-NHS were purchased from Shanghai yuanye Bio-Technology Co., Ltd. Phosphate buffered saline (PBS, pH 7.4) was purchased from Biological Industries. Pluronic F-127 was purchased from Beyotime biotechnology Co., Ltd. Poly (DL-lactic-co-glycolic acid) (PLGA) and 1-ethyl-3-(3-dimethylaminopropyl) carbodiimide (EDC) were purchased from the Shanghai Macklin Biochemical Technology Co., Ltd. Horseradish Peroxidase (HRP) was purchased from the Solarbio Science & Technology Co., Ltd (Beijing). Citrate Buffer and Chloroauric acid (48–50% Au basis) ($HAuCl_4$) were purchased from the Shanghai Macklin Biochemical Technology Co., Ltd. The cyclic RGD (cyclic Arg-Gly-Asp-D-Tyr-Lys) peptide was purchased from Xi'an Ruixi Biological Technology Co., Ltd. Hydroxylamine hydrochloride was purchased from Tianjin chemical reagent factory.

2.2 Fabrication of TP-Au-RGD nanoparticles

Under magnetic stirring, 300 mg of PLGA and 18 mg of TP were dissolved in 30 ml of dichloroethane, and slowly added drop-wise 300 ml of distilled water containing Pluronic F-127 (300 mg) as a stabilizer to the above solution. The mixture was emulsified by ultrasonication for 1 h after mixing the oil and water phase, then following evaporation of dichloroethane with stirring for 24h. Then, the TP-PLGA nanoparticles were collected by centrifugation, and then re-dispersed in 10 ml of PBS through sonication. After that, the TP-PLGA nanoparticles solution was added to 50 mL Au nanoparticles (AuNps) solution with vigorously stirred for 20 h. Then, the TP-PLGA-AuNps nanoparticles were collected by centrifugation.

The sodium citrate reduction method is used to prepare AuNps [19]. 64 ml of 0.1 g/L $HAuCl_4$ solution is heated to boiling. Then the solution stirred strongly at around 120rpm, meanwhile, 0.42 ml of 10 g/L sodium citrate are added dropwise into the solution to keep the reduction time about 6min. After that, the solution is kept boiling until the solution turns red–purple and transferred into a flask and then stored at 4°C before use. Then, 0.315 mL sodium citrate solution and 22.592 mL of $HAuCl_4$ solution were added to 60 mL TP-PLGA-AuNps under ultrasonic stirring. Afterwards, hydroxylamine solution was added drop by drop and the mixed solution was stirred for 30 min to realize the reduction of $HAuCl_4$ under the ultrasonication. The formation of Au nanoshell outside the TP-PLGA nanoparticles was by the reducing $HAuCl_4$ around TP-PLGA-AuNps [19].

The TP-PLGA-Au nanoparticles were dispersed into SH-PEG-COOH solution by sonication from the substrate and collected by centrifugation at 10000 rpm. Under magnetic stirring, the collected carboxylate-terminated TP-PLGA-Au nanoparticles, cyclic RGD (6 mg), 8 mg of NHS and 8 mg of EDC

were dispersed in 18 mL of PBS (0.2 M, pH 7.4) at room temperature. During this period, the RGD peptides is covalently bound to the -COOH group of the SH-PEG-COOH chains adsorbed to Au nanoshell. TP-Au-RGD nanoparticles were collected by centrifugation after 24 h, discarded the supernatant that contained unreacted cyclic RGD. Finally, the obtained TP-Au-RGD nanoparticles were freeze-dried and stored.

2.3 Synthesis of thiol and tyramine modified HA

Synthesis of thiol and tyramine modified HA as show in Fig. 2a. HA (0.5 g) was dissolved in 100 ml of deionized water. 0.958 g of EDC and 0.575 g of NHS (5 mmol) were released in deionized water (10 ml), and add to the above HA solution, respectively. The mixture was adjusted pH to 5.4 with 1 M HCl and then stirred 0.5 h. After that, 1.74 g of TA (10 mmol) and 2.25 g of cystamine dihydrochloride (10 mmol) were added to the mixture and then stirred 24 h. 2.3 g of DTT (15 mmol) was added and stirred 24 h. Transferred the mixture solution into a dialyzed for 3 days to ensure the remaining tyramine hydrochloride and other salts completely removed. The cut off molecular weight of dialysis bag is 3.5 k Da. and then. Finally, the obtained -SH and tyramine modified HA was freeze-dried.

2.4 Preparation of TP-Au/HA hybrid hydrogels

The preparation of the hybrid hydrogel refers to the previous work [29]. -SH and tyramine modified HA (0.5 g) was dissolved in 10 ml of PBS at room temperature. After completely dissolved, gently mixed 10 mg of TP-Au-RGD nanoparticles to the prepared solutions and ultrasonication for 10 min. Subsequently, HRP was dissolved in PBS (50 µl, 0.02 mg/ml)was added to the previous mixture first, then hydrogen peroxide (H_2O_2) (50 µl, 0.02wt %). The mixture was then stirred gently, which resulted in hydrogels formation. The obtained TP-Au/HA hybrid hydrogels was freeze-dried.

2.5 Material characterization

The obtained TP-Au-RGD nanoparticles were characterized by a ^{1}HNMR spectrometer (Varian Gemini-300, DMSO-d_6). The zeta-potential and size of obtained TP-Au-RGD nanoparticles were measured by dynamic light scattering at 25°C. The TP-Au-RGD nanoparticles exhibited an average size of 140.3 nm. The zeta potential was found to be − 15.2 ± 0.4 mV. The TP-Au-RGD nanoparticles using TEM was shown is Fig. 2b. The encapsulation efficiency of the prepared TP-Au-RGD nanoparticles were found to be 30 ± 5%.

2.6 In vitro release

Initially, 10 mg of TP-Au/HA hybrid hydrogels and equivalent TP-Au-RGD nanoparticles were loaded into two separate dialysis bag, the cut off molecular weight of dialysis bag is 1k Da. The two separate dialysis bag were immersed in a small glass containing with 10 mL of PBS and slight constant shaking at150 rpm, respectively. And NIR irradiation of 0.53 W/cm^2 for 10 min performed at beginning. Due to maintain release conditions, using fresh PBS to replace the release medium at determined intervals to at 37 ℃. Using UV-vis spectrophotometry to measure the amount of released TP at 220 nm.

2.7 RA-FLSs preparation and culturing

RA-FLSs and growth medium were purchased from Cell Applications (Beijing Longyue Biological Technology Development Co., Ltd.). RA-FLS cells obtained from passages 5 to 9 were seeded onto 96-well plates at a density of 1 x 10^4 cells /mL. They were cultured in Dulbecco's modified Eagle medium (DMEM) with 4.5 g/L glucose, 100 μg/mL streptomycin, 100 IU/ml penicillin, and 10% fetal bovine serum. Cells were grown in a humidified 37 ℃ incubator with oxygen and 5% CO_2 .

2.8 CCK-8 assay

A CCK-8 assay was used to measure the effect of TP-Au/HA hybrid hydrogels on the proliferation of RA-FLSs. In brief, RA-FLSs were collected and seeded onto 96-well plates at a density of 2 × 10^4 cells/well. Then, the cells were plates with different concentration of drug and for different lengths of time (24 h, 48 h). Cells were treated with TP solution (0.13 and 30μM), TP-Au/HA hybrid hydrogels with equivalent TP of o.13μM without NIR irradiation, and TP-Au/HA hybrid hydrogels with equivalent TP of o.13μM with NIR irradiation (0.38 W/cm^2 for 10 min). After the treatments, 10 μl CCK-8 solution (Shanghai yuanye Bio-Technology Co., Ltd.) was added to each well and incubated at 37 ℃, and 5% CO^2 for 1 h. The absorbance was determined at 450 nm by using an enzyme-linked immunosorbent assay reader (BioTek Instruments, Inc., Winooski, VT, USA).

2.9 Western blot analysis

mTOR、p-mTOR、p70S6Kand p-p70S6K protein (Abcam, UK) expression was evaluated by western blotting. Extracts of total protein cell were prepared by the Cell Lysis Buffer (Abcam, UK). Each sample was loaded thirty micrograms of total protein and separated on a 4–20% SDS–PAGE gel under reducing conditions. Then, transferred the samples onto a nitrocellulose membrane, and then blocked in 5% nonfat dry milk. The membranes were incubated with primary antibodies and secondary antibodies. Detection was performed using chemiluminescence.

2.10 Induction and treatment of CIA mice

Firstly, bovine type II collagen (200μg, Sigma-Aldrich, Shanghai) emulsified in complete Freund's adjuvant (200μg, Sigma-Aldrich, Shanghai) was intravenous injection male DBA/1J mice (8 weeks old, Medcona, China) to induce rheumatoid arthritis, which using an intradermal injection. Next, 100μg of bovine type II collagen in incomplete Freund's (Sigma-Aldrich, Shanghai) was given at 21 days after the primary immunization, which using a booster intradermal injection.

After rheumatoid arthritis was fully developed, saline (G1), TP solution (G2), TP-Au/HA hybrid hydrogels (G3 and 4) were intraarticular administered to the mice, and after TP-Au/HA hybrid hydrogels injection, G4 combined with10 min 1.59 W/cm^2 NIR light (n = 5 mice each group). Mice were monitored twice a week for 4 weeks after intra-articular injection. The clinical index is the amount of the clinical scores for four-paw clinical scores, the highest score is 16 points [30]. The evaluated paws were scored from 0 to 4 according to the following scale: 0 = no erythema and swelling, 1 = erythema and mild swelling, 2 = erythema and mild swelling extending from the tarsals to the ankle, 3 = erythema and moderate swelling

extending from the metatarsal to ankle joints, and 4 = erythema and severe swelling of the digits, foot and ankle or ankylosis of the limb.

2.11 In vivo NIR imaging

TP-Au/HA hybrid hydrogels were intraarticular injected into the CIA mice (200 μ L, 1mg/ml dispersed in PBS). The mice were anesthetized with a short acting anesthetic, and kept during the imaging process. IVIS Spectrum (Carestream Health Fx Pro/FX) in vivo fluorescence imaging system was used.

2.12 Histological examination

The mice were sacrificed after 28 days of each treatment. Removed the joints from the mice, and fixed in 10% buffered formalin saline at 4°C for 1 week for histopathological examination. The decalcified joints were embedded in paraffin blocks and 4μm-thick paraffin sections were sliced. Using hematoxylin and eosin (H&E) to stain the joint tissues sections, and score the changes in synovial inflammation on a scale of 0–4 [33]. Each score was assessed by two independent experimenters and the average grades were calculated.

2.13 Microcomputed Tomography

Experimental mice paws of each groups were scanned by micro-CT system (SkyScan 1176, SkyScan, Aartselaar, Belgium). Images were acquired at 80 k Vp, 5 s/frame, and 150 mA, with 360 views. The estimated radiation dose was approximately 6.9 mGy using image acquisition protocol. Using NFR Polarys software (Exxim Computing Corporation, Pleasanton, USA) to reconstruct and evaluate the three-dimensional structure of scanned paws., And using Aquarius software (version 4.4.6, TeraRecon, Inc.) to measure three-dimensional bone volume (BV) including phalanges and metatarsal bones to confirm volumetric change of arthritis joints.

2.14 Biodistribution and clearance

TP-Au/HA hybrid hydrogelswere administered intraarticularly into CIA mice (200μL, 1mg/ml dispersed in PBS) (n = 5).The mice were sacrificed after 28 days of each treatment, and removed the major organs (liver, heart, spleen, kidney and lung) from the mice.

2.15 Statistical analyses

All images and data were from three independent experiments. Data are expressed as means ± standard deviation. Statistical analyses of group were performed using the Prism graph pad 8.0, and post-test was

followed by Tukey's method.

3. Results And Discussion

3.1 Preparation and characterization of TP-Au/HA hybrid hydrogels

The preparation route is shown in Fig. 1. First, we prepared TP-PLGA nanoparticles. Next, through the electrostatic interaction, TP-PLGA nanoparticles were modified with AuNps orderly to obtain TP-PLGA-AuNps nanoparticles, and $HAuCl_4$ is reduced around TP-PLGA-AuNps to form Au nanoshell outside the TP-PLGA nanoparticles [19]. AuNps were prepared in boiling condition by reducing and stabilizing $HAuCl_4$ with sodium citrate [30]. And the TP-PLGA-Au nanoparticles were dispersed into 1 wt % SH-PEG-COOH solution by sonication, and then collected by centrifugation. The cyclic RGD peptide for targeted delivery can bind $R_v\beta_3$ expressed on angiogenic vascular endothelial cells at inflammatory sites [31]. The size of bare TP-Au-RGD nanoparticles was 140.3 nm in diameter. The zeta potential was found to be − 15.2 ± 0.4. ^1H NMR spectra of the obtained TP-Au-RGD nanoparticles was examined in Fig. 3b, peaks at 8.27–8.438 ppm correspond to the -NH(NH_2) = NH of cyclic RGD and 4.85–5.02 ppm correspond to the CH of PLGA. The absorption peak of AuNPs at 680 nm to 740 nm in the UV-vis-NIR spectra (Fig. 3c), indicating that Au nanoshell was formatted and nanoparticles can be used for NIR absorbance imaging and photothermal therapy in vivo.

For the preparation of the modified HA, hydroxylic groups of hyaluronic acid were activated by HCl and then reacted with tyramine and cystamine [10]. This process resulting in the formation of a carbamate bond between the amine group of HA and the hydroxyl groups, and end-group thiolated HA was synthesized via reductive amination, as shown in Fig. 2a. ^1H NMR spectra of the modified HA was showed in Fig. 3a. The new appeared peaks at 6.64 and 6.60 ppm corresponded to the aromatic protons of TA being integrated, and peaks of two methylene groups on cysteamine were at 2.05 and 2.67 ppm. Finally, through the catalysis of H_2O_2 and HRP, tyramines and thiol oxidatively coupled to form the hydrogels. The SEM images of modified HA showed the surface morphology is smooth in Fig. 2c. The TEM image was evident that TP-Au-RGD nanoparticles were homogenous distributed in the hydrogels in Fig. 2d, and the SEM image of hydrogels in Fig. 2e

3.2 Drug release and photothermal effects

In vitro release studies, we measured the release of TP-Au/HA hybrid hydrogels and TP-Au-RGD nanoparticles, which demonstrated longer sustained delivery of drug from the higher cross-linking hydrogels. A relatively dense and stable hydrophilic shell was formed by the long HA chain with multiple interaction sites, as shown in Fig. 1a. TP-Au-RGD nanoparticles showed that the release time of TP is 3 days, and the burst release is more than 60% within 12 h (Fig. 4c). The release profile of drug from TP-Au/HA hybrid hydrogels showed the sustained release time of TP is 3 days, and the burst release of

about 60% of the drug within 72h, which may be related to the embedding of nanoparticles within hydrogels network. The release from TP-Au/HA hybrid hydrogels was slower, which might be related to the combined efficacy of TP-Au-RGD nanoparticles release and coacervate system [32]. After the degradation of HA chains, the surface of the TP-Au-RGD nanoparticles was exposed to the surrounding environment [22, 29]. Because the Au nanoshell has absorption in the NIR region, NIR irradiation will locally generate heat which is not enough to cause irreversible tissue damage [33]. And with increasing temperature, the degradation of biodegradable PLGA nanoparticles was more rapidly [34, 35]. Then, we measured the release rate of TP at 37°C to study the efficacy of NIR irradiation and non-NIR irradiation (Fig. 4d). The release profile of TP from TP-Au-RGD nanoparticles with non-NIR irradiation is in a linear, showing the release rate of TP was nearly constant. However, the release rate was reduced and induced a burst release of TP for 12h with 10 min NIR irradiation. These results indicate that NIR irradiation can control the TP release rate from TP-Au-RGD nanoparticles.

3.3 The proliferation inhibition effect on RA-FLSs in vitro study

In vitro study, we used RA-FLSs to confirm photothermal controlled release of drugs and anti-inflammatory effects of the TP-Au/HA hybrid hydrogels combined with NIR irradiation. CCK-8 assay demonstrated that the proliferation of RA-FLSs was significantly inhibited by TP-Au/HA hybrid hydrogels (Fig. 5d). G1 was a control group. And G2 and G3 were treated with 0.13μM and 30μM TP solutions, respectively. G4 and G5 were prepared by culturing cells with TP-Au/HA hybrid hydrogels (equivalent TP of G2) for 1 day. And G5 was also treated with 10 min NIR irradiation at 0.38 W/cm^2. As expected, due to the lower TP concentration, the cell anti-proliferation effect of G2 was much less than G3. The treatment of TP-Au/HA hybrid hydrogels significantly enhance cell anti-proliferation without NIR irradiation (G4). The greatest anti-proliferation effect of cell was the treatment of TP-Au/HA hybrid hydrogels combined with NIR irradiation (G5), although the dosage of TP in G5 was lower than G3. These results demonstrated that TP-Au/HA hybrid hydrogels had a synergistic effect with NIR irradiation.

3.4 Effects of TP-Au/HA hybrid hydrogels on the mTOR/p70S6K signaling pathway

The distinctive feature of RA are synovial inflammation and synovial cell hyperplasia [36]. RA-FLSs, the key components of the invasive synovium, play an important role in the initiation and perpetuation of destructive joint inflammation [37]. The important chemokines (CXCL1, CXCL5,, G-CSF, etc.), inflammatory cytokines (TNF-a, IL-1b, IL-6, etc.) and inflammatory mediators (TLR-2, TLR-4, iNOS, etc.) released by RA-FLSs can promote the infiltration of DCs, monocytes, neutrophils, macrophages, B cells and T cells into joints, which lead to the chronic inflammation and joint destruction [36]. Recent studies have demonstrated that the mammalian target of rapamycin/p70 ribosomal protein S6 kinase (mTOR/p70S6K) signaling pathway has a major role in regulating cell survival and apoptosis, which is over-activated in RA-FLSs, as in Fig. 5a [38]. mTOR is upregulated in a variety of cancers and regulates cancer cell invasion, and its expression also related to the poor prognosis in cancer [24, 37, 39–42]. It is

well known that the 70 k Da ribosomal S6 kinase p70S6K1 regulates cell growth by inducing protein synthesis components [40]. Considering this background information, we hypothesized that the apoptosis-inducing effect of hybrid hydrogels on RA-FLSs might be correlated with the inhibition of the mTOR/p70S6K signaling pathway. Therefore, we analyzed the protein expressions levels of total mTOR、p70S6K、p-mTOR、p-p70S6K in the each group by western blotting analysis (Fig. 5b and Fig. 5c). The results showed that hydrogels-treated with RA-FLSs, which were exposed to 10 min NIR irradiation at 0.38 W/cm^2 after administered, the levels of phosphorylated mTOR had significantly reduced (Fig. 5b, phospho-mTOR/total median reduction of 54%), as well as reduced the level of a phosphorylated form of one mTOR substrate, p70S6K (Fig. 5c, phospho-p70S6K/total median reduction of 38%), confirms that the inhibition of this pathway is correlated with reduction of apoptosis. These data indicated that hybrid hydrogels can inhibit the mTOR/p70S6K signaling pathway in RA-FLSs.

3.5 In vivo targeted effects and NIR imaging

CIA mice were generated to evaluate the targeted effects and NIR imaging of TP-Au/HA hybrid hydrogels on inflammatory joints in vivo. These mice were intraarticular injected with TP-Au/HA hybrid hydrogels solution (200μl). Because of superior capabilities of Au nanoshell, the hybrid hydrogels will lead to composite systems of hydrogels with unique optical properties [43, 44]. The injected hybrid hydrogels were monitored in vivo NIR absorbance at 5min and 24h (Fig. 4a). We noted that the color of the inflammatory paws was changing, while observed the color of noninflammatory paws was not obvious changing, which indicated that nanoparticles were selectively delivered to the inflammatory areas and accumulated in the inflammatory joints. Meanwhile, we noted the color of the inflamed paw of CIA mice changing over time because of the localization of TP-Au-RGD nanoparticles in the inflammatory paws (Fig. 4b). These results indicated that TP-Au-RGD nanoparticles were preferentially delivered to the inflammation region by active targeting, rather than passive targeting, and accumulated in the inflammatory paws effectively.

3.6 In vivo efficacy

In order to study the treatment efficacy of hybrid hydrogel, divide CIA mice into four groups (n = 5 mice each group) with intraarticular administration, as summarized in Table 1. Figure 4e shows the clinical index of these groups over time. 35 mg/kg TP was injected intraarticularly four times a week (G2) as a positive control. Compared to the mice treated with saline (G1), other groups showed the decrease of clinical indices observed with some variations depending on the day. In G3, the decrease of clinical indices was slow until about day 20 and then increased, which the mice treated with TP-Au/HA hybrid hydrogels (0.2 mg/kg) with non-NIR irradiation, though they were lower than G1. However, may be due to photothermally controlled drug release, the clinical indices of G4 were lower than G2, which the administration of CIA was the TP-Au/HA hybrid hydrogels (0.2 mg/kg) combined with 10 min 1.59 W/cm^2 NIR irradiation. As shown in Fig. 4d, the release of TP for G3 is slow; therefore, the lack of NIR light impeded the sustained release of TP, resulting in the poor irradiation effects. In contrast, when the inflammatory paws exposed to NIR light (G4), the release of more than 10% of the TP within 12 h (Fig. 4d), which is a much lower TP dosage than G2 and obtained high therapeutic effect. These results

indicate that photothermal-chemo therapy using TP-Au/HA hybrid hydrogels is a good way in the treatment of RA, which can maximize irradiation efficacy and reduce dose-related TP side effects.

Tablw 1
Group of CIA mice

Group	Administered content	Dosage of TP (mg/kg)	NIR light (W/cm^2)
1	saline		
2	TP solution	35 × 4 times	
3	TP-Au/HA hybrid hydrogels	0.2	
4	TP-Au/HA hybrid hydrogels	0.2	1.59

Administrated content was injected intraarticularly by volume 200μL. The joints was exposed to NIR light for 10 min with 1.59 W/cm ^{2} after injection.

3.7 Histopathological evaluation

To confirm the effects of the targeted photothermal-chemo treatment, joints histological examinations were performed 28 days after intraarticular injection (Fig. 6a). Severe infiltration of inflammatory cell was showed in the joint sections of untreated mice. The infiltration of inflammatory cell was significantly reduced in mice injected with TP solution four times a week (G2) and TP-Au/HA hybrid hydrogels with NIR irradiation (G4). In contrast, significant differences were not observed in G3 mice (Fig. 6b).

3.8 CT imaging

We performed three-dimensional micro-CT to assess bony changes in the paws of CIA mice (Fig. 6c). The severe bone destruction of paws, which treated CIA mice with saline. The bone structures of G2 and G4 were relatively well preserved. The bone volume of the paws of CIA mice was measured to determine the extent of bone preservation. The bone volume of the paws tended to be better preserved, which treated with TP-Au/HA hybrid hydrogels and NIR irradiation (Fig. 6d). These results indicated that the therapeutic effect of TP-Au/HA hybrid hydrogels with NIR irradiation is comparable to conventional TP treatment.

3.9 In vivo toxicity of TP-Au/HA hybrid hydrogels

Histological examinations of major organs (liver, spleen, lung, kidney and heart) were performed 28 days after injection to investigate the influence of TP-Au/HA hybrid hydrogels on the major organs (Fig. 4f). G4 showed no apparent tissue damage compared to the healthy control group, demonstrating that the TP-Au-RGD nanoparticles did not accumulated in major organs and induce toxicity in vivo.

4. Conclusions

In summary, we demonstrate the synergistic therapeutic effects of TP-Au/HA hybrid hydrogels with chondroprotection, anti-inflammation, photothermal-chemo therapy and in vivo imaging for the treatment of RA. When the hybrid hydrogels were administrated into the joints, the in vivo NIR absorbance images showed that the nanoparticles can selective accumulate in the inflammation areas of CIA mice. The release rate of TP from the hybrid hydrogels has accelerated because of NIR irradiation, allowing the photothermal-chemo therapy. Compared to conventional single treatment with TP, the treatment of TP-Au/HA hybrid hydrogels combined with NIR irradiation had excellent treatment effects with a smaller dosage of TP and low toxicity. Furthermore, the findings suggested that TP-Au/HA hybrid hydrogels inhibited inflammation via suppressing the invasion and migration of RA-FLSs, by blocking the phosphorylation of the mTOR/p70S6K pathway at least in part. The result demonstrates that the targeted photothermal-chemo therapy using hybrid hydrogels in the treatment of RA is an effective strategy that can maximize the therapeutic effects and reduce dose-related side effects.

Declarations

ACKONWLEDGMENTS

Not applicable.

FUNDING

This work was supported by Beijing Natural Science Foundation (7202111), National Science and Technology Major Project (2018ZX10101001-005-003). All special thanks for the long-term subsidy mechanism from the Ministry of Finance and the Ministry of Education of PRC for BUCM.

AUTHOR CONTRIBUTIONS

Yuanyan Liu: provided the concept and designed the study. Chenxi Li: performed the experiments, analyzed the data wrote the manuscript. Rui Liu, Yurong Song, Dongjie Zhu contributed to the rearing of mice. Liuchunyang Yu Qingcai Huang, Zeyu Xue, Zhengjia Zhang, and Zhenglai Hua contributed to culture cells. Cheng Lu supervised the projected. All authors discussed the results and revised the manuscript.

AVAILABILITY OF DATA AND MATERIALS

All data generated or analyzed during this study are included in this published article and supplementary information files.

Ethics approval and consent to participate

All animal experiments were conducted under the Ethical and Regulatory Guidelines for Animal Experiments defined by Institute of Basic Theory, China Academy of Chinese Medical Sciences (License Number: SCXK (Beijing) 2016-0011, SYXK (Beijing) 2017-0033).

Consent for publication

All authors agreed to submit this manuscript.

Competing interests

The authors declare that they have no competing interests as defined by *Journal of Nanobiotechnology*, or other interests that might be perceived to influence the results and discussion reported in this paper.

References

1. Smolen JS, Aletaha D, McInnes IB. Rheumatoid arthritis. The Lancet. 2016;388:2023–38.
2. Ha YJ, Lee SM, Mun CH, Kim HJ, Bae Y, Lim JH, Park KH, Lee SK, Yoo KH, Park YB. Methotrexate-loaded multifunctional nanoparticles with near-infrared irradiation for the treatment of rheumatoid arthritis. Arthritis Res Ther. 2020;22:146.
3. Yang Y, Ye Y, Qiu Q, Xiao Y, Huang M, Shi M, Liang L, Yang X, Xu H. Triptolide inhibits the migration and invasion of rheumatoid fibroblast-like synoviocytes by blocking the activation of the JNK MAPK pathway. Int Immunopharmacol. 2016;41:8–16.
4. Li Y, Wang J, Xiao Y, Wang Y, Chen S, Yang Y, Lu A, Zhang S. A systems pharmacology approach to investigate the mechanisms of action of Semen Strychni and Tripterygium wilfordii Hook F for treatment of rheumatoid arthritis. J Ethnopharmacol. 2015;175:301–14.
5. Zhou ZL, Yang YX, Ding J, Li YC, Miao ZH. Triptolide: structural modifications, structure-activity relationships, bioactivities, clinical development and mechanisms. Nat Prod Rep. 2012;29:457–75.
6. Li P, Yang X, Yang Y, He H, Chou CK, Chen F, Pan H, Liu L, Cai L, Ma Y, Chen X. Synergistic effect of all-trans-retinal and triptolide encapsulated in an inflammation-targeted nanoparticle on collagen-induced arthritis in mice. J Control Release. 2020;319:87–103.
7. Cai XJ, Fei WD, Xu YY, Xu H, Yang GY, Cao JW, Ni JJ, Wang Z. Combination of metronomic administration and target delivery strategies to improve the anti-angiogenic and anti-tumor effects of triptolide. Drug Deliv Transl Res. 2020;10:93–107.
8. Mousavi Nejad Z, Torabinejad B, Davachi SM, Zamanian A, Saeedi Garakani S, Najafi F, Nezafati N. Synthesis, physicochemical, rheological and in-vitro characterization of double-crosslinked

hyaluronic acid hydrogels containing dexamethasone and PLGA/dexamethasone nanoparticles as hybrid systems for specific medical applications. Int J Biol Macromol. 2019;126:193–208.

9. Agas D, Laus F, Lacava G, Marchegiani A, Deng S, Magnoni F, Silva GG, Di Martino P, Sabbieti MG, Censi R. Thermosensitive hybrid hyaluronan/p(HPMAm-lac)-PEG hydrogels enhance cartilage regeneration in a mouse model of osteoarthritis. J Cell Physiol. 2019;234:20013–27.
10. Kurisawa M, Chung JE, Yang YY, Gao SJ, Uyama H. **Injectable biodegradable hydrogels composed of hyaluronic acid-tyramine conjugates for drug delivery and tissue engineering**. *Chem Commun (Camb)* 2005:4312–4314.
11. Burdick JA, Prestwich GD. Hyaluronic acid hydrogels for biomedical applications. Adv Mater. 2011;23:H41–56.
12. Annapoorna SVAS, Subramania MRJ, Shantikumar I. VN, R J: Injectable deferoxamine nanoparticles loaded chitosan-hyaluronic acid coacervate hydrogel for therapeutic angiogenesis. Colloids Surf B Biointerfaces. 2018;161:129–38.
13. Arun Kumar R, Sivashanmugam A, Deepthi S, Iseki S, Chennazhi K, Nair S, Jayakumar R. Injectable Chitin-Poly(ε-caprolactone)/Nanohydroxyapatite Composite Microgels Prepared by Simple Regeneration Technique for Bone Tissue Engineering. ACS Appl Mater Interfaces. 2015;7:9399–409.
14. Vaca-Gonzalez JJ, Clara-Trujillo S, Guillot-Ferriols M, Rodenas-Rochina J, Sanchis MJ, Ribelles JLG, Garzon-Alvarado DA, Ferrer GG. Effect of electrical stimulation on chondrogenic differentiation of mesenchymal stem cells cultured in hyaluronic acid - Gelatin injectable hydrogels. Bioelectrochemistry. 2020;134:107536.
15. Li C, Cao Z, Li W, Liu R, Chen Y, Song Y, Liu G, Song Z, Liu Z, Lu C, Liu Y. A review on the wide range applications of hyaluronic acid as a promising rejuvenating biomacromolecule in the treatments of bone related diseases. Int J Biol Macromol. 2020;165:1264–75.
16. Faust HJ, Sommerfeld SD, Rathod S, Rittenbach A, Ray Banerjee S, Tsui BMW, Pomper M, Amzel ML, Singh A, Elisseeff JH. A hyaluronic acid binding peptide-polymer system for treating osteoarthritis. Biomaterials. 2018;183:93–101.
17. Racine L, Guliyeva A, Wang I, Larreta-Garde V, Auzely-Velty R, Texier I. **Time-Controllable Lipophilic-Drug Release System Designed by Loading Lipid Nanoparticles into Polysaccharide Hydrogels**. *Macromol Biosci* 2017, 17.
18. Zhao F, Yao D, Guo R, Deng L, Dong A, Zhang J. Composites of Polymer Hydrogels and Nanoparticulate Systems for Biomedical and Pharmaceutical Applications. Nanomaterials (Basel). 2015;5:2054–130.
19. Liu X, Gao C, Gu J, Jiang Y, Yang X, Li S, Gao W, An T, Duan H, Fu J, et al. Hyaluronic Acid Stabilized Iodine-Containing Nanoparticles with Au Nanoshell Coating for X-ray CT Imaging and Photothermal Therapy of Tumors. ACS Appl Mater Interfaces. 2016;8:27622–31.
20. Rao KM, Kumar A, Suneetha M, Han SS. pH and near-infrared active; chitosan-coated halloysite nanotubes loaded with curcumin-Au hybrid nanoparticles for cancer drug delivery. Int J Biol Macromol. 2018;112:119–25.

21. Shakeri-Zadeh A, Zareyi H, Sheervalilou R, Laurent S, Ghaznavi H, Samadian H. Gold nanoparticle-mediated bubbles in cancer nanotechnology. Journal of controlled release: official journal of the Controlled Release Society. 2021;330:49–60.
22. Hien NQ, Van Phu D, Duy NN. Quoc le A: **Radiation synthesis and characterization of hyaluronan capped gold nanoparticles**. Carbohydr Polym. 2012;89:537–41.
23. Kim H, Park Y, Stevens MM, Kwon W, Hahn SK. Multifunctional hyaluronate - nanoparticle hybrid systems for diagnostic, therapeutic and theranostic applications. J Control Release. 2019;303:55–66.
24. Laragione T, Gulko PS. mTOR regulates the invasive properties of synovial fibroblasts in rheumatoid arthritis. Mol Med. 2010;16:352–8.
25. Bottini N, Firestein GS. Duality of fibroblast-like synoviocytes in RA: passive responders and imprinted aggressors. Nat Rev Rheumatol. 2013;9:24–33.
26. Dai Q, Zhou D, Xu L, Song X. Curcumin alleviates rheumatoid arthritis-induced inflammation and synovial hyperplasia by targeting mTOR pathway in rats. Drug Des Devel Ther. 2018;12:4095–105.
27. Wu X, Long L, Liu J, Zhang J, Wu T, Chen X, Zhou B, Lv TZ. Gambogic acid suppresses inflammation in rheumatoid arthritis rats via PI3K/Akt/mTOR signaling pathway. Mol Med Rep. 2017;16:7112–8.
28. Feng FB, Qiu HY. Effects of Artesunate on chondrocyte proliferation, apoptosis and autophagy through the PI3K/AKT/mTOR signaling pathway in rat models with rheumatoid arthritis. Biomed Pharmacother. 2018;102:1209–20.
29. Kheirabadi M, Shi L, Bagheri R, Kabiri K, Hilborn J, Ossipov DA. In situ forming interpenetrating hydrogels of hyaluronic acid hybridized with iron oxide nanoparticles. Biomater Sci. 2015;3:1466–74.
30. Lee M, Yang J, Jung H, Beack S, Choi J, Hur W, Koo H, Kim K, Yoon S, Hahn S. Hyaluronic acid-gold nanoparticle/interferon α complex for targeted treatment of hepatitis C virus infection. ACS Nano. 2012;6:9522–31.
31. Hynes R. A reevaluation of integrins as regulators of angiogenesis. Nature medicine. 2002;8:918–21.
32. Jin KM, Kim YH. Injectable, thermo-reversible and complex coacervate combination gels for protein drug delivery. J Control Release. 2008;127:249–56.
33. Laroui H, Grossin L, Léonard M, Stoltz J, Gillet P, Netter P, Dellacherie E. Hyaluronate-covered nanoparticles for the therapeutic targeting of cartilage. Biomacromol. 2007;8:3879–85.
34. Park H, Yang J, Lee J, Haam S, Choi I, Yoo K. Multifunctional nanoparticles for combined doxorubicin and photothermal treatments. ACS Nano. 2009;3:2919–26.
35. Zolnik BS, Leary PE, Burgess DJ. Elevated temperature accelerated release testing of PLGA microspheres. J Control Release. 2006;112:293–300.
36. Tang Y, Liu Q, Feng Y, Zhang Y, Xu Z, Wen C, Zhang Y. Tripterygium Ingredients for Pathogenicity Cells in Rheumatoid Arthritis. Front Pharmacol. 2020;11:583171.

37. Pantuck AJ, Seligson DB, Klatte T, Yu H, Leppert JT, Moore L, O'Toole T, Gibbons J, Belldegrun AS, Figlin RA. Prognostic relevance of the mTOR pathway in renal cell carcinoma: implications for molecular patient selection for targeted therapy. Cancer. 2007;109:2257–67.
38. Huang Y-Y, Jiang H-X, Shi Q-Y, Qiu X, Wei X, Zhang X-L, Qin S-Y: ** miR-145 Inhibits Th9 Cell Differentiation by Suppressing Activation of the PI3K/Akt/mTOR/p70S6K/HIF-1α Pathway in Malignant Ascites from Liver Cancer **. *OncoTargets and Therapy* 2020, **Volume 13**:3789–3800.
39. An JY, Kim KM, Choi MG, Noh JH, Sohn TS, Bae JM, Kim S. Prognostic role of p-mTOR expression in cancer tissues and metastatic lymph nodes in pT2b gastric cancer. Int J Cancer. 2010;126:2904–13.
40. Zhou F, He X, Iwakura Y, Horai R, Stuart JM. Arthritis in mice that are deficient in interleukin-1 receptor antagonist is dependent on genetic background. Arthritis Rheum. 2005;52:3731–8.
41. Zhou L, Huang Y, Li J, Wang Z. The mTOR pathway is associated with the poor prognosis of human hepatocellular carcinoma. Med Oncol. 2010;27:255–61.
42. Meng Q, Xia C, Fang J, Rojanasakul Y, Jiang BH. Role of PI3K and AKT specific isoforms in ovarian cancer cell migration, invasion and proliferation through the p70S6K1 pathway. Cell Signal. 2006;18:2262–71.
43. Ye E, Loh XJ. Polymeric Hydrogels and Nanoparticles: A Merging and Emerging Field. Aust J Chem. 2013;66:997.
44. Shin K, Ryu K, Lee H, Kim K, Chung H, Sohn D. Au nanoparticle-encapsulated hydrogel substrates for robust and reproducible SERS measurement. Analyst. 2013;138:932–8.

Figures

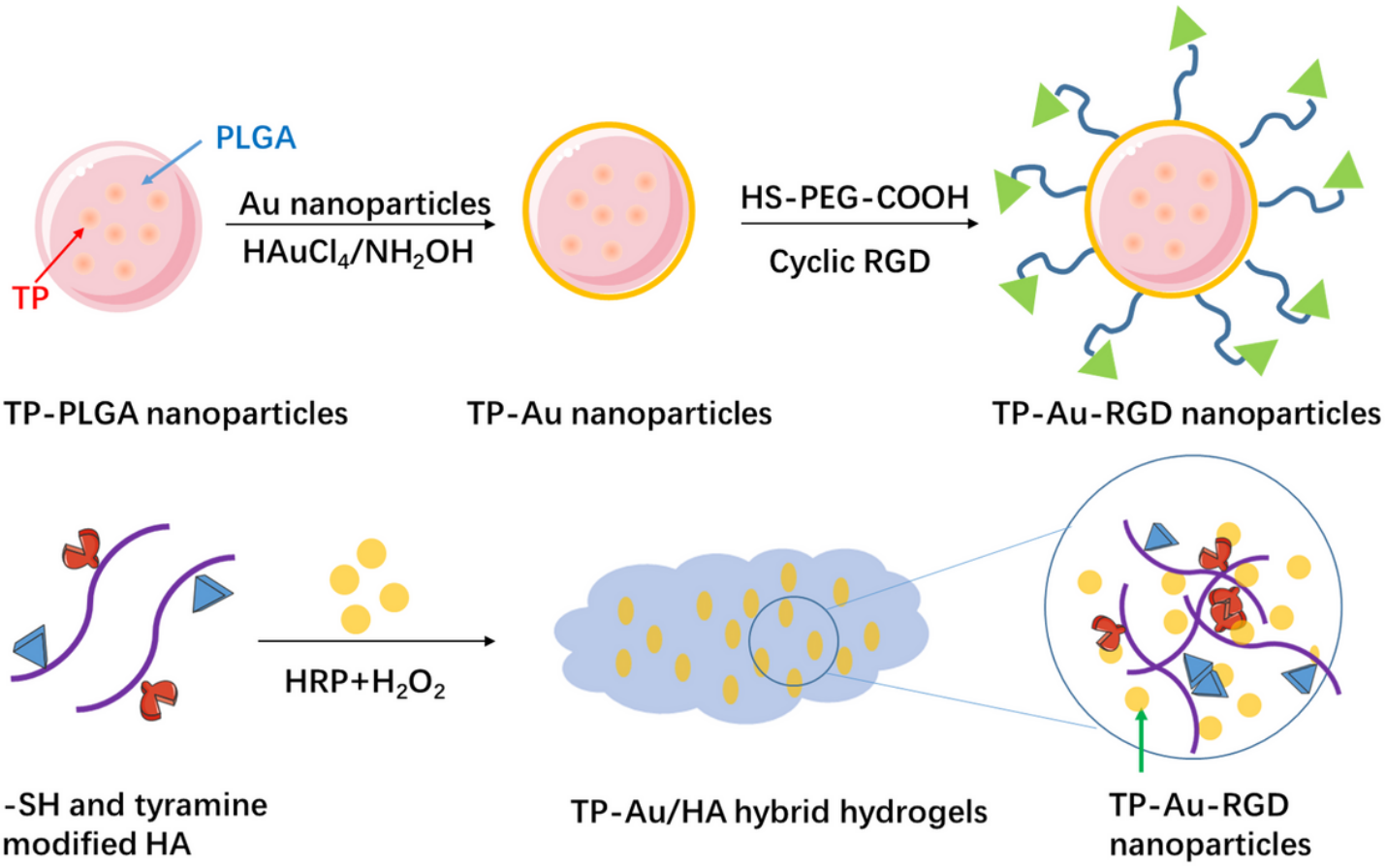

Figure 1

The preparation route of TP-Au/HA hybrid hydrogels.

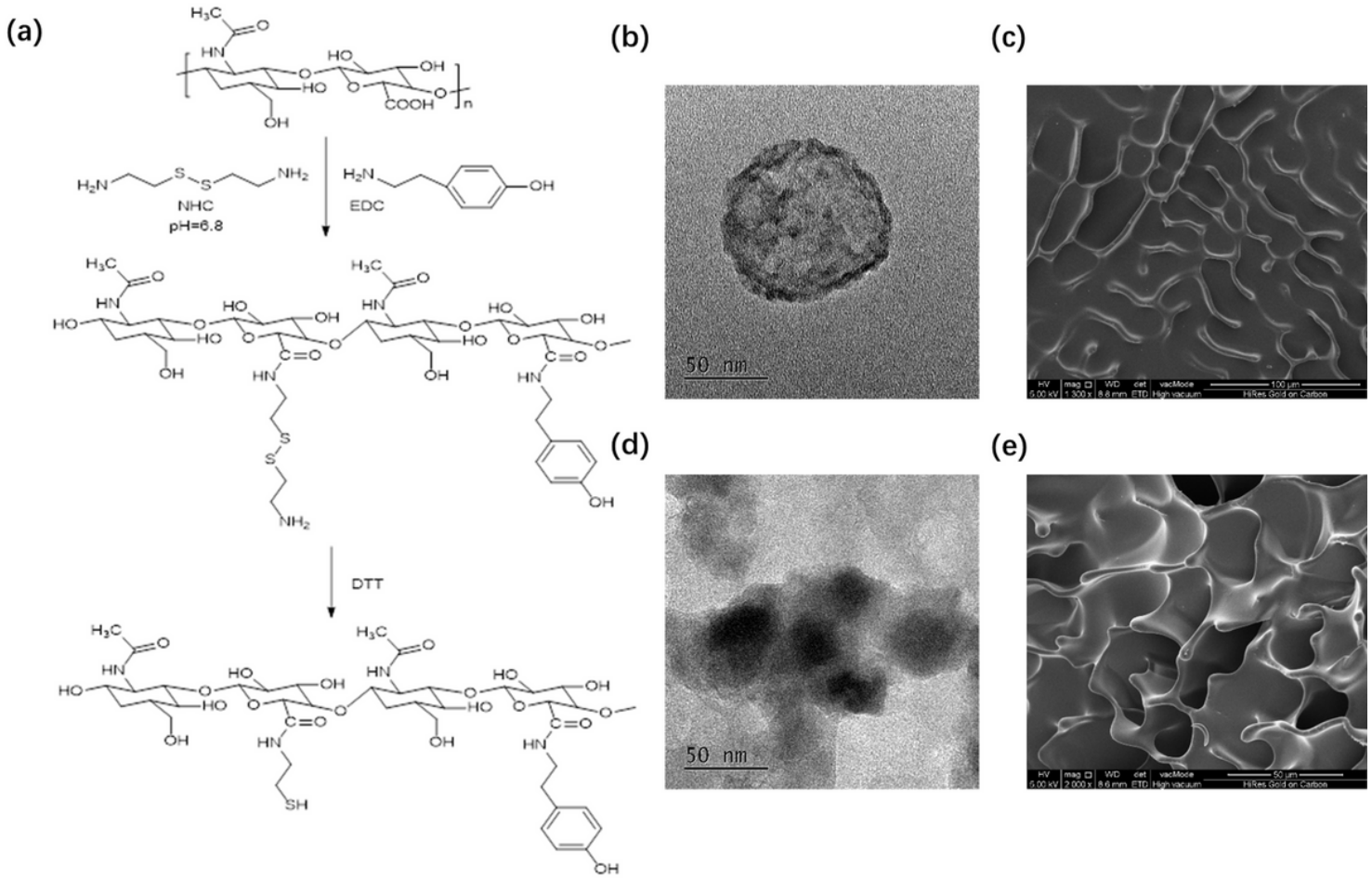

Figure 2

(a) Synthesis of thiol and tyramine modified HA. (b) TEM image of TPAu-RGD nanoparticles. (c) SEM image of modified HA. (d) TEM image was evident that TP-Au-RGD nanoparticles were embedded within the hydrogels matrix. (e) SEM image of TP-Au/HA hybrid hydrogels.

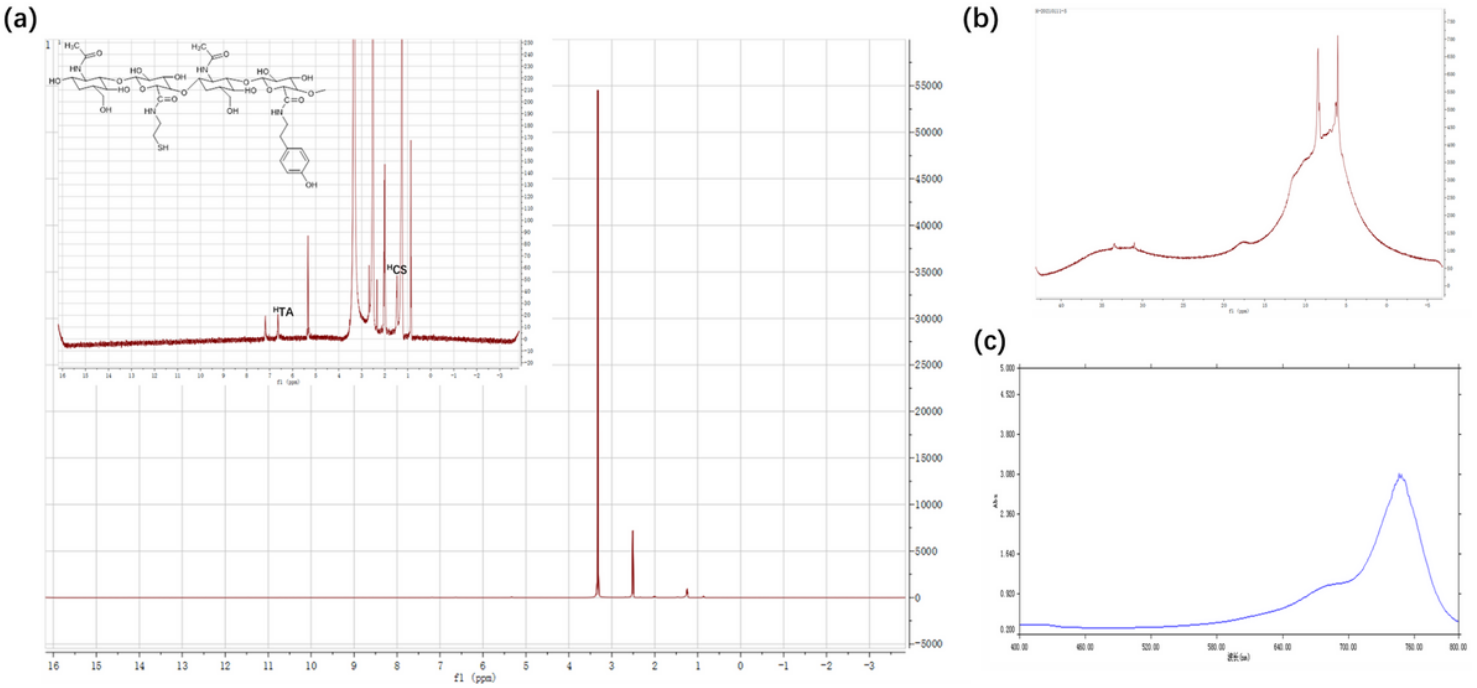

Figure 3

(a) 1H NMR spectra of modified HA. (b) 1H NMR spectra of TP-Au-RGD nanoparticles. (c) UV-vis-NIR absorbance spectra of Au nanoshell.

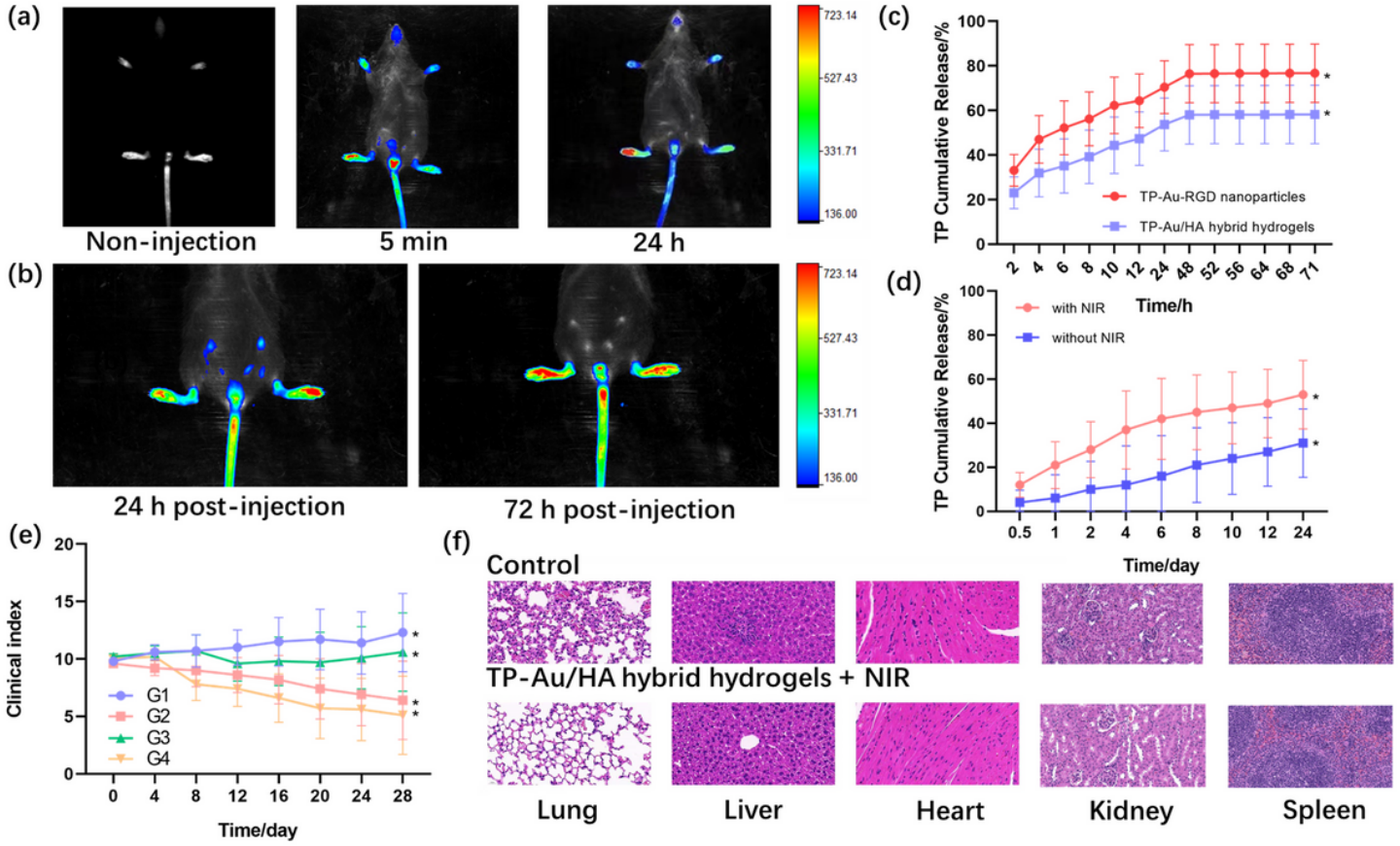

Figure 4

(a) In vivo NIR absorbance images of inflammatory and non-inflammatory paws in CIA mouse injected intraarticularly with TP-Au/HA hybrid hydrogels (200μL,1mg/mL dispersed in PBS) (Left paws are non-inflammatory and right paws are inflammatory). (b) In vivo NIR absorbance images of inflammatory paws of CIA mouse after intraarticular injection of TP-Au/HA hybrid hydrogels (the picture below is a 4× magnification). (c) Profiles of TP release from TP-Au/HA hybrid hydrogels and TP-Au-RGD nanoparticles with NIR irradiation of 0.53 W/cm2 for 10 min at the initial time. (d) Profiles of TP release from TP-Au-RGD nanoparticles with and without NIR irradiation of 0.53 W/cm2 for 10 min at the initial time. Data represent mean values for n = 3, and the error bars represent standard deviation of the means (*p < 0.05). (e) Clinical index versus time for CIA mice injected intraarticularly. Clinical indices were significantly different among groups (*p < 0.05). (f) Histological sections of major organs extracted 28 days after intraarticular injection of TP-Au/HA hybrid hydrogels with NIR irradiation or healthy mice. Images were at 20×magnification.

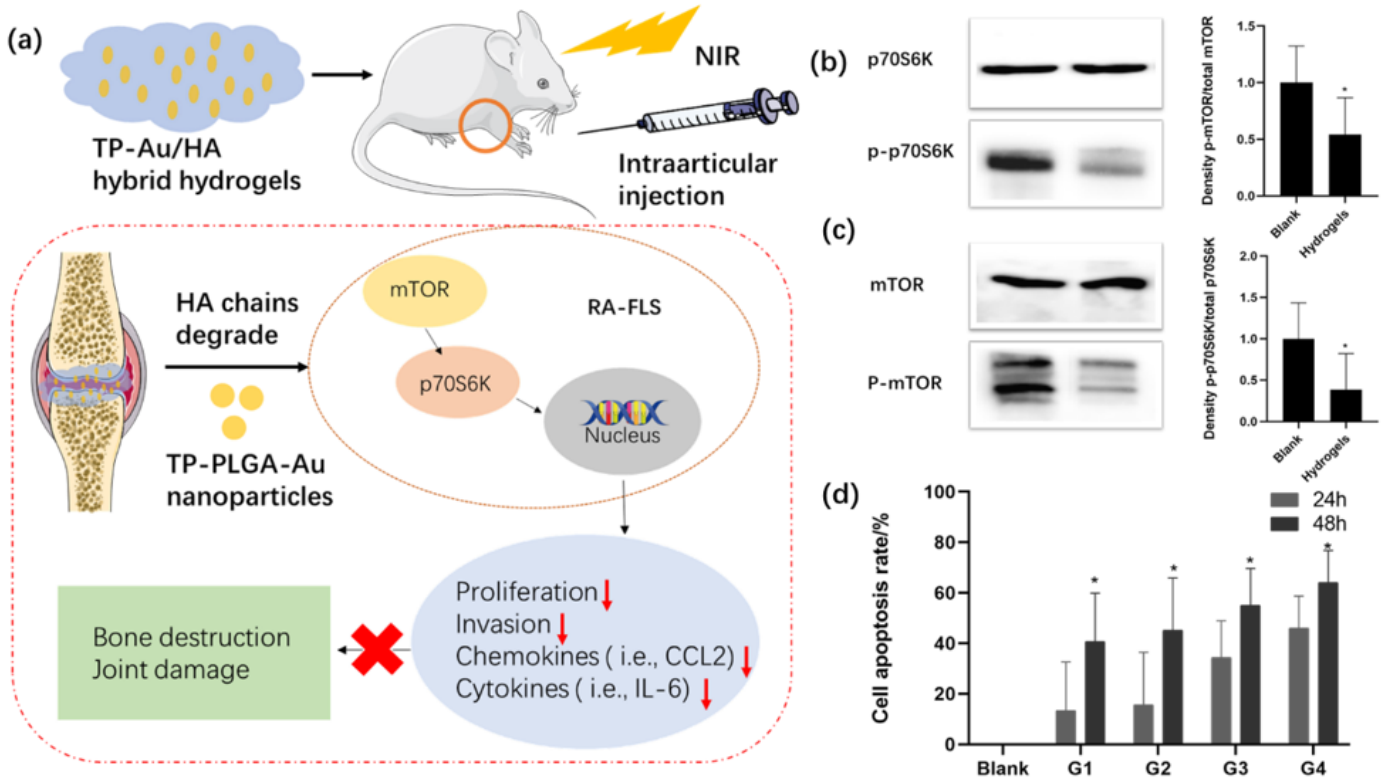

Figure 5

(a) Schematic illustration of anti-inflammatory effect of TP-Au/HA hybrid hydrogels in mouse CIA model. (b) TP-Au/HA hybrid hydrogels reduced levels of phospho-mTOR, with a phospho-mTOR/total median reduction of 54% and (c) Levels of phosphorylation of mTOR targets phospho-p70S6K (phospho-p70S6K/total median reduction of 38%, confirms that the inhibition of this pathway. (d) Effect of TP-Au/HA hybrid hydrogels on the anti-proliferation of RA-FLSs. The data are expressed as the mean ± SEM values. By comparison with blank group,*P□0.05.

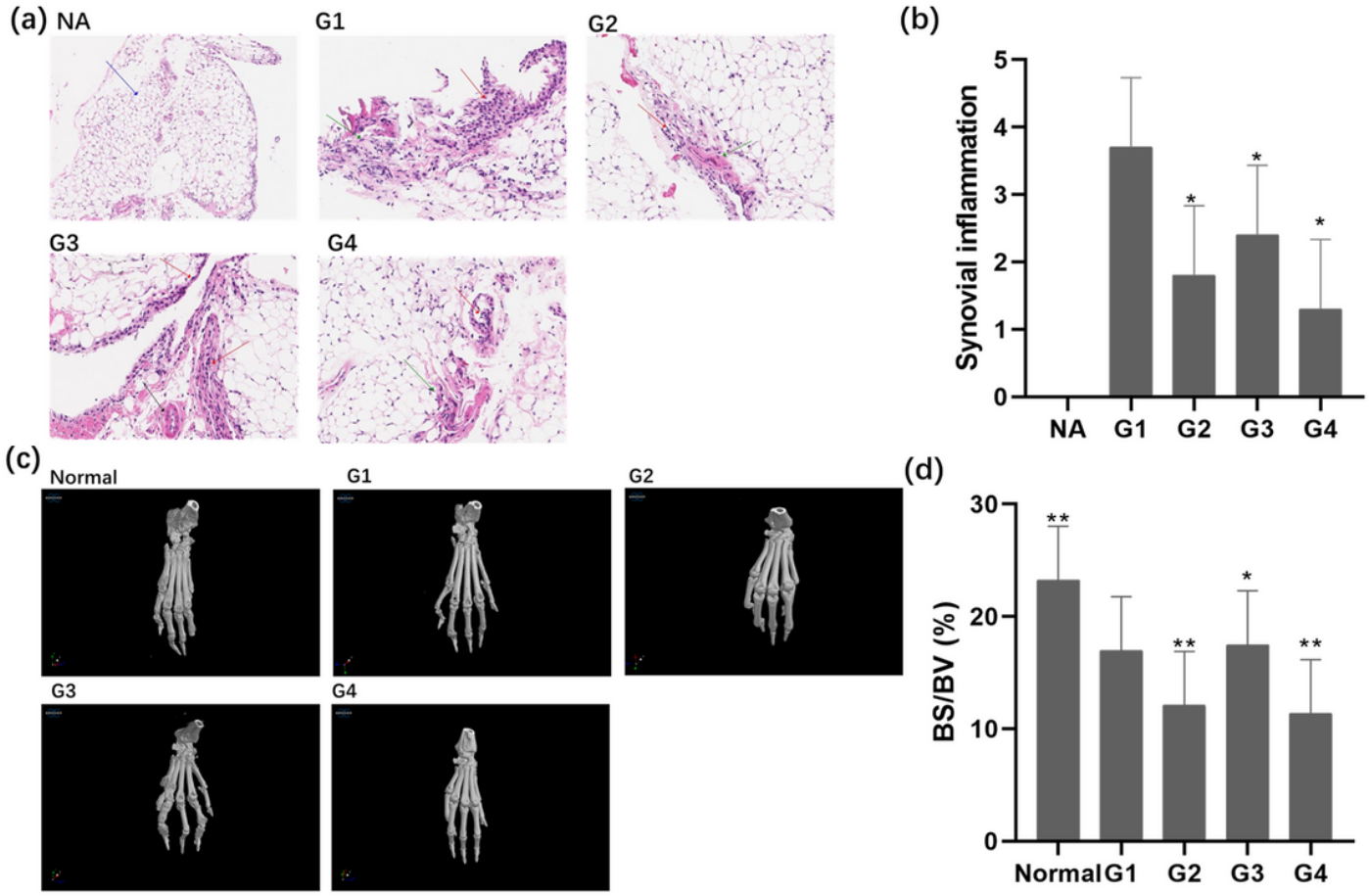

Figure 6

(a) Synovial inflammation from CIA mice and normal mice (NA) 28 days after treatment, H&E (100×original magnifications). (b) Semiquantitative analysis of synovial inflammation. *p < 0.05 (n = 5). (c) Micro-computed tomography images of paws of CIA mice in different group. (b) Effects of TP-Au/HA hybrid hydrogels on bone destruction in CIA mice. Bone surface/volume ratio (BS/BV; %). * p < 0.05 versus G1; ** p < 0.01 versus G1.

Supplementary Files

This is a list of supplementary files associated with this preprint. Click to download.

- GraphicalAbstract.tif